The Cryosphere, 7, 241–248, 2013
www.the-cryosphere.net/7/241/2013/
doi:10.5194/tc-7-241-2013

The Cryosphere
Open Access

Brief communication
"Important role of the mid-tropospheric atmospheric circulation in the recent surface melt increase over the Greenland ice sheet"

X. Fettweis[1], **E. Hanna**[2], **C. Lang**[1], **A. Belleflamme**[1], **M. Erpicum**[1], **and H. Gallée**[3]

[1]Laboratory of Climatology, Department of Geography, University of Liège, n°2 Allé du 6 Aout, 4000, Liège, Belgium
[2]Department of Geography, University of Sheffield, Winter Street, S10 2TN, Sheffield, UK
[3]Laboratoire de Glaciologie et Géophysique de l'Environnement (LGGE), n°54 Rue Molir̂e, 38402, Grenoble, France

Correspondence to: X. Fettweis (xavier.fettweis@ulg.ac.be)

Received: 13 July 2012 – Published in The Cryosphere Discuss.: 24 September 2012
Revised: 14 January 2013 – Accepted: 15 January 2013 – Published: 7 February 2013

Abstract. Since 2007, there has been a series of surface melt records over the Greenland ice sheet (GrIS), continuing the trend towards increased melt observed since the end of the 1990s. The last two decades are characterized by an increase of negative phases of the North Atlantic Oscillation (NAO) favouring warmer and drier summers than normal over GrIS. In this context, we use a circulation type classification based on daily 500 hPa geopotential height to evaluate the role of atmospheric dynamics in this surface melt acceleration for the last two decades. Due to the lack of direct observations, the interannual melt variability is gauged here by the summer (June–July–August) mean temperature from reanalyses at 700 hPa over Greenland; analogous atmospheric circulations in the past show that ∼ 70 % of the 1993–2012 warming at 700 hPa over Greenland has been driven by changes in the atmospheric flow frequencies. Indeed, the occurrence of anticyclones centred over the GrIS at the surface and at 500 hPa has doubled since the end of 1990s, which induces more frequent southerly warm air advection along the western Greenland coast and over the neighbouring Canadian Arctic Archipelago (CAA). These changes in the NAO modes explain also why no significant warming has been observed these last summers over Svalbard, where northerly atmospheric flows are twice as frequent as before. Therefore, the recent warmer summers over GrIS and CAA cannot be considered as a long-term climate warming but are more a consequence of NAO variability affecting atmospheric heat transport. Although no global model from the CMIP5 database projects subsequent significant changes in NAO through this century, we cannot exclude the possibility that the observed NAO changes are due to global warming.

1 Introduction

Since 2007, a succession of summers with record surface melt rates has been observed over the Greenland ice sheet (GrIS) (Tedesco et al., 2008a,b, 2011, 2012; Rignot et al., 2011; Box et al., 2012; Hanna et al., 2012), coinciding with minimums in the Arctic sea ice cover (Serreze et al., 2007; Comiso et al., 2008). Except for 2009, the surface melt over 2007–2012 summers is unprecedented in the last 50 yr reanalysis-forced reconstructions (Van den Broeke et al., 2009; Fettweis et al., 2011b; Tedesco et al., 2011, 2012). Recent melt records agree with a trend of increased melt over the GrIS, which has been observed since the end of the 1990s (Mote, 2007; Fettweis et al., 2011b) and attributed to increased atmospheric greenhouse gas concentration (Fettweis, 2007; Hanna et al., 2008). This trend has also been observed in the Canadian Arctic Archipelago (CAA) where the 2005–2009 melt was four times greater than the 1995–2000 mean (Gardner et al., 2011; Sharp et al., 2011; Fisher et al., 2012). But, no significant warming has been observed since 2004 over Svalbard located 500 km to the east of the GrIS. As a result, the increased mass loss rate observed from 1996 (Bamber et al., 2005) was no longer observed after 2004, and more recent Svalbard elevation change has been closer to zero (Moholdt et al., 2010).

The 2007–2012 warming recently observed over the GrIS did not occur everywhere in the Arctic because it was mainly driven by anomalies in the atmospheric dynamics locally impacting the heat transport (Mote, 1998; Graversen et al., 2008). These general circulation anomalies come from changes in the North Atlantic Oscillation (NAO) variability as pointed out by Chylek et al. (2004), Fettweis et al. (2011a), Box et al. (2012) and Hanna et al. (2012). Indeed, the last six summers were characterized by persistent negative NAO modes, favouring warmer and more anticyclonic (drier) conditions than normal over the GrIS (Box et al., 2012; Hanna et al., 2012) but, conversely, by normal conditions over Svalbard, as we will see later.

Therefore, in this paper we evaluate the role of the atmospheric dynamics in the 1993–2012 melt increase over GrIS and more generally of the warming of the atmosphere just over the GrIS surface (here at 700 hPa) in summer with the help of

– a Circulation Type Classification (CTC) that extracts the main regimes of the mid-tropospheric general circulation. This allows us to show the changes in the atmospheric dynamics explaining the recent melt records over the GrIS;

– a flow-analogue method that enables us to estimate the part of the warming due to changes in atmospheric dynamics. This estimation is achieved by reconstructing the climate of the last 20 summers with the help of analogue flows (i.e. similar tropospheric patterns) which occurred during the 1961–1990 summers (our reference period). In theory, if we assume that the more recent 1993–2012 warming was solely driven by changes in atmospheric circulation, an equivalent warming should be reconstructed by replacing the current daily climate with that taken from the dates of analogous flows in the past.

2 The last two decades over Greenland in a longer-term perspective

As shown in Fig. 1a, the June–July–August (JJA) meltwater production over the GrIS has been increasing since 1995 and is without precedent in 1998, 2003, 2007, 2008, and 2010–2012 compared with the last 50 yr. Over the last 20 yr (1993–2012), the amount of melt has doubled compared with 1961–1990. Results from the regional climate model MAR (Fettweis et al., 2011b) forced by ERA-40 (1958–1978, Uppala et al., 2005) and ERA-INTERIM (1979–2012, Dee et al., 2011) reanalyses from the European Centre for Medium Range Weather Forecasts (ECMWF) are used here because no observations of meltwater production are available at the scale of the whole ice sheet. Only the melt extent can be derived from satellite (Fettweis et al., 2011b; Hanna et al., 2012) but, while melt extent and meltwater production are

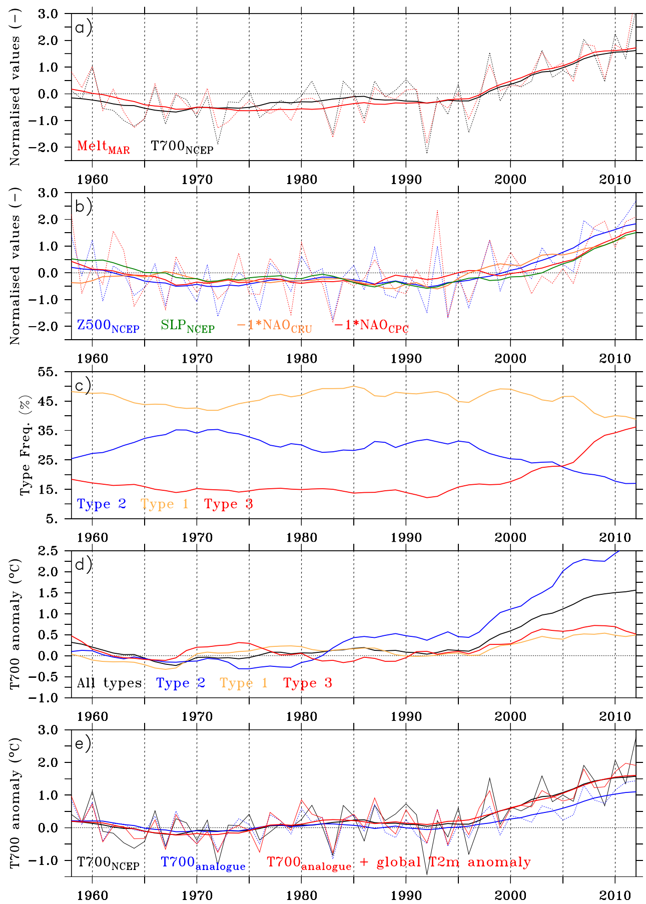

Fig. 1. (a) Normalised time series of the annual GrIS melt amount simulated by MAR (in red) and of the JJA T700 averaged over the area covering Greenland (20° W ≤ longitude ≤ 70° W and 60° N ≤ latitude ≤ 85° N) from the NCEP-NCAR reanalysis (in black). The smoothed lines show the 10-yr running mean of the time series. **(b)** Normalised time series of the JJA Z500 averaged over the area covering Greenland (in blue), of the JJA SLP (in green), of the Z500 based NAO index (in red) from the Climate Prediction Center (CPC) of the National Oceanic and Atmospheric Administration (NOAA) and of the SLP-based NAO index (in orange) from the Climate Research Unit (CRU). Here the sign of the NAO indexes time series has been changed to be consistent with the other time series. **(c)** Evolution (in percentage) of the number of occurrences of each circulation class shown in Fig. 3 for each summer from 1958 to 2012. A 10-yr running mean is applied here. **(d)** Time series in °C of the JJA T700 averaged over the area covering Greenland (in black) and of the T700 averaged over the days contained in each type of the CTC. Only 10-yr running means are shown here. The same figure using a 3-yr running mean is provided in the Supplement. Anomalies are relative to the 1961–1990 baseline period. **(e)** Time series in °C of the JJA T700 averaged over the area covering Greenland (in black), of the analogues-based T700 (in blue) and of the analogues-based T700 plus the anomaly of the global annual NCEP-NCAR 2-m-temperature (in red) compared with the 1961–1990 mean.

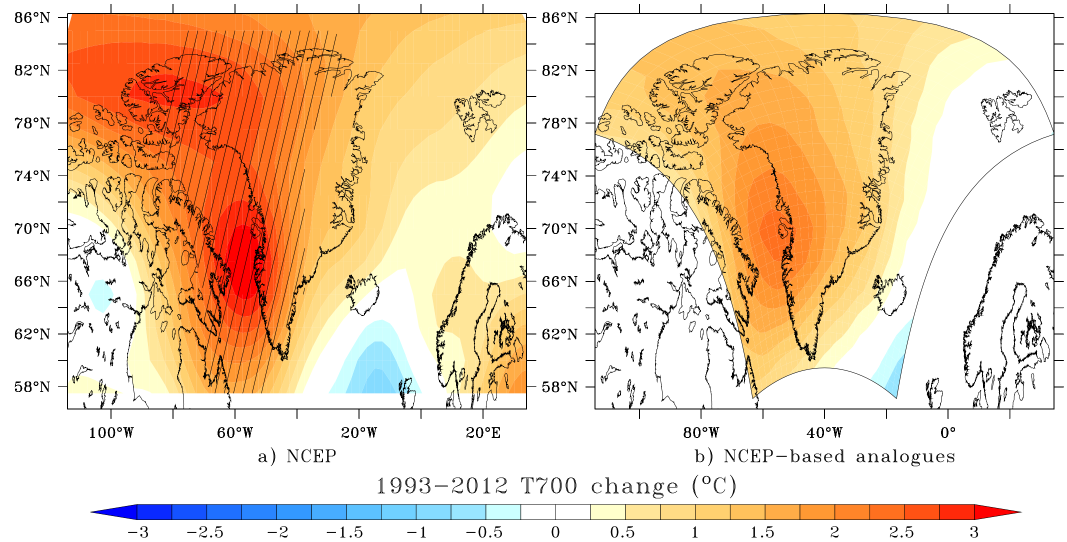

Fig. 2. (a) The JJA T700 changes over 1993–2012 based on a linear regression using the NCEP-NCAR reanalysis. The areas where the changes are two times above the 1961–1990 JJA T700 standard deviation are hatched. **(b)** The same as **(a)** but derived using the NCEP-NCAR-based T700 analogues.

highly correlated (Fettweis et al., 2006), melt extent cannot be used as a direct proxy of meltwater production. Indeed, for the same melt extent, the amount of meltwater can be very different and depends on the presence and extent of bare ice zones (which have a lower albedo and higher melt rate than melting snow) in the melt area. The ability of MAR to simulate the melt extent has been shown in Fettweis et al. (2011b).

Apart from being affected by the surface albedo or the inertia of the snowpack, the melt amount is driven by the atmospheric temperature and, therefore, the temperature at 700 hPa (T700) is an excellent proxy for explaining the melt variability. Indeed, the MAR-based meltwater production variability is highly correlated (correlation coefficient of 0.93) with JJA T700 from the Reanalysis version 1 (Kalnay et al., 1996) of the National Centers for Environmental Prediction (NCEP) and the National Center for Atmospheric Research (NCAR) averaged over an area covering the GrIS (20° W $\leq$ longitude $\leq 70^\circ$ W and 60° N $\leq$ latitude $\leq 85^\circ$ N). Let us remember that MAR is forced by the ECMWF reanalysis. The correlations are lower (< 0.9) for NCEP-NCAR temperatures taken at lower vertical levels than 700 hPa. Knowing that the temperature in the free atmosphere depends directly on the atmospheric dynamics, we will discuss hereafter the recent warming at 700 hPa over Greenland instead of the surface melt increase itself (see Fig. 1a).

In parallel with enhanced melt since the end of the 1990s, we observe an increase of the JJA geopotential height at 500 hPa (Z500) and the JJA sea level pressure (SLP) over the GrIS due to the increased occurrence of negative NAO phases in recent summers (see Fig. 1b). This means that the atmospheric dynamics in summer is currently more anticyclonic (both at the surface and at 500 hPa) over GrIS than 20 yr ago. This configuration tends to favour warm air advection over the west side of the GrIS due to weaker Icelandic lows (Fig. 2a), as found by Hanna et al. (2012). Indeed, most of the significant temperature increase has occurred along the western coast of Greenland and over the CAA. Along the eastern coast, over the adjacent part of the North Atlantic Ocean and over Svalbard, the temperature changes are not statistically significant (Fig. 2a). This regional disparity of warming agrees with trends from climate station records presented by Hanna et al. (2012).

The Z500, T700, SLP used here come from the NCEP-NCAR reanalysis over 1958–2012. To check the sensitivity of our results to the choice of a particular dataset, we produced similar figures to Figs. 2 and 3 but this time based on the ECMWF ERA-40 (1958–1978) and ERA-INTERIM (1979–2012) reanalyses – see Supplement – although it is noted that the ECMWF-based time series (composed of two different reanalyses) is not homogeneous. In summer for example, T700 over GrIS is lower in ERA-40 than in ERA-INTERIM over the common period (1979–2001) (Fettweis et al., 2012). Such discrepancies impact the analogue-based reconstruction because ERA-40 based T700 is used to reconstruct the current ERA-INTERIM based T700.

3 Methodology

3.1 Circulation type classification

The automatic CTC method used here is adapted from the approach of Lund (1963), i.e. our CTC characterises each pair of days by a similarity index based on the daily Z500 and uses it afterwards to group days with similar circulations

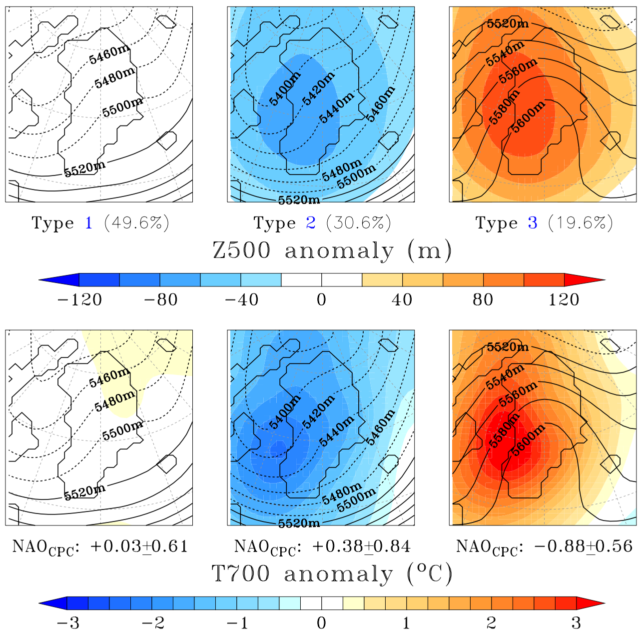

Fig. 3. (Top) The Z500 average over the days categorized into the 3 classes minus the JJA Z500 average over the whole period 1958–2012. The solid lines ($Z500 > 5500$ m) and the dashed lines ($Z500 \geq 5500$ m) denote the Z500 type-average. For each circulation type, the proportion of days contained in that class compared to the 5060 days of the 1958–2012 JJA months is indicated in brackets. (Below) The lower panels show much the same but for T700. The daily mean NAO index from CPC when the considered circulation type occurs is listed. Both Z500 and T700 fields come here from the NCEP-NCAR reanalysis.

(Philipp et al., 2010). In the original classification of Lund (1963), the correlation between the SLP surfaces is used to evaluate the similarity between two days. Here, in view of the GrIS topography, it is better to use the Z500 surfaces (the ice sheet top reaches an altitude above that of the 700 hPa pressure plane). The correlation-based index treats two parallel but distant Z500 surfaces as similar because they have the same pattern. However, if the Z500 surfaces are at different heights, this means that the temperature of the troposphere below 500 hPa is different. Therefore, these two Z500 surfaces will not have the same impact on the surface melt and then, they cannot be considered as similar in our case. Hence our similarity index is as well a function of the euclidean distance between the two Z500 surfaces, which gives more weight to the height of the Z500 surfaces in our CTC. Fettweis et al. (2011a) showed that the melt variability over the GrIS is driven more by the height of the Z500 surfaces than their pattern. We refer to Fettweis et al. (2011a) for more details about our CTC and the choice of our index. The only difference with Fettweis et al. (2011a) is the domain which has been enlarged here to include Svalbard and Ellesmere islands. In addition, the number of circulation types allowed in our CTC (fixed to eight in Fettweis et al., 2011a) is here set to three, to distinguish only neutral (i.e. close to the climatological mean), cyclonic and anticyclonic regimes.

3.2 Flow analogues

The flow-analogue method, used here for estimating the JJA temperature anomalies at 700 hPa induced by the general circulation, is similar to that of Vautard and Yiou (2009), i.e. for each JJA day of the 1958–2012 period, flow analogues are selected in a 30-day window centred on this given day but not in the same year. This means that the analogues of the 1st of July 1958 are looked for between the 16 June and the 15 July from other summers than 1958. As for the CTC, our similarity index (defined in the previous section) is used to select the most similar Z500 surfaces to a given day. Its value is chosen to have analogues in at least ten different summers to avoid an abnormal summer being "described" by another abnormal summer. Thereby, the analogues properly represent the average climate corresponding to a Z500 surface for a given date. With this aim, it is clear that the flow-analogue method cannot represent exceptional climate anomalies. In addition, since the aim is to estimate the impact of the atmospheric dynamics on the last 20 yr melt variability over the GrIS, analogues are only taken from the 1961–1990 summers. The daily analogue T700 is then defined as the median of daily T700 from the analogue days. As shown in Table S1 of the Supplement, our results are not significantly affected by the different parameters fixed in our methodology (i.e. using analogues in at least 5 or 15 summers instead of 10; 20-day or 40-day window instead of 30-day window; mean instead of the median of the analogue T700; daily anomalies instead of raw values; analogues taken in the 1958–2012 summers instead of 1961–1990). The uncertainties given in our analogues-based results were derived using the different configurations listed above.

4 Changes in atmospheric dynamics

The three main atmospheric circulation regimes extracted by our CTC are shown in Fig. 3 as Z500 anomalies with respect to the JJA Z500 mean. As Z500 depends on the atmospheric temperature below 500 hPa, the pattern of the corresponding T700 anomalies in each circulation type is obviously correlated to the Z500 one while, as we will show later, T700 does not drive our CTC. The main circulation types found by our automatic CTC are a type (no. 1) close to the JJA climatology induced by neutral NAO conditions; a cyclonic type (no. 2) induced by positive NAO conditions, and an anticyclonic type (no. 3) gauged by negative NAO phases. On average over the period 1958–2012, Type no. 1 occurs 50 % of the JJA time, while only 20 % of JJA daily circulations at 500 hPa are classified as anticyclonic (Type no. 3).

For the mid-1960s to mid-1990s, both CRU and CPC JJA NAO indexes are on average positive (see Fig. 1b), indicating more frequent cyclonic circulations at the expense of anticyclonic regimes. Before 1965, slightly negative NAO conditions prevailed on average, favouring anticyclonic types (see Fig. 1c), but those negative NAO phases are insignificant compared with those occurring since 2000. Indeed, over the last two decades, there has been a significant frequency increase (from ∼ 15 % to ∼ 40 %) of daily circulations classified as anticyclonic Type no. 3. This type favours warmer conditions over Greenland by advecting warm air masses along its western coast. However, since the atmospheric temperature impacts the geopotential height, the increase of occurrence of Type no. 3 could be an artefact driven by the atmospheric temperature increase over the last 20 yr. Figure 1d shows that such a temperature increase occurs for each type of the CTC, indicating that the variability of our circulation regimes is independent of the current warming. Moreover, the same CTC based on SLP instead of Z500 shows that there is also an increase of anticyclonic conditions at the surface, which similarly favours warmer atmospheric conditions in West Greenland (see Fig. S4a, b in the Supplement).
Therefore, such an increase in the occurrence of anticyclonic conditions (both at the surface and altitude) is not an artefact of our methodology and is in agreement with the statistically significant temperature increase since the 1990s over Greenland and the neighbouring Canadian islands (see Fig. 2). Over Svalbard, the increasing occurrence of anticyclones centred over Greenland favours northerly flows inducing temperatures rather near the normal, in agreement with Kvamsto et al. (2012) who showed that the highest temperatures over Svalbard were reached at the beginning of the 2000s.

5 Atmospheric dynamics induced warming

By using the flow analogues technique, we can evaluate the part of the currently observed warming over GrIS which is induced by anomalies in atmosphere dynamics independently of the anthropogenic radiative forcing.

If we use a similarity index only computed over the area (described earlier) covering the GrIS, the correlation between the daily Z500 surfaces averaged over this area and the corresponding Z500 analogues-based ones are 0.99 with a RMSE of 13.2 m, knowing that the standard deviation of the daily area-averaged Z500 surfaces is 74.2 m. This good comparison at a daily time scale validates to some extent our flow analogues technique. We refer to the Supplement for a comparison in two dimensions (see Fig. S5a, b in the Supplement). Such an agreement also shows that the Z500 surfaces from the last two decades are not exceptional because analogues can successfully be found in the past. But let us remember that the occurrence of the anticyclone-like Z500 surfaces during the recent 2007–2012 summers is exceptional.
For T700 averaged over this area, the correlation with the daily analogues-based T700 is 0.86 with a RMSE of 1.2 °C given that the standard deviation of the daily area-averaged T700 is 2.3 °C over 1993–2012. The comparison is worse for T700 than Z500 since for a same Z500 surface, T700 can be very different depending on whether there is a low or a high pressure at the surface and on the temperature gradient in the airmass below 500 hPa. In addition, bearing in mind that the climate is currently warming due to the anthropogenic radiative forcing, the T700 associated with a Z500 surface was generally lower 20 yr ago than currently (Fig. 1d).

Figures 1e and 2b show the T700 increase induced by the changes in the general circulation using analogues from 1961–1990. The pattern of Fig. 2a is well reproduced by the analogues but the temperature increase is underestimated. Indeed, averaged over Greenland and after having applied a 10-yr running mean, the analogues explain only 69 ± 4 % (resp. 65 ± 5 %) of the reanalysis-based 1993–2012 (resp. 1983–2012) JJA warming at 700 hPa (see Fig. 1d). The linear trend of JJA T700 is 0.1 °C/summer (resp. 0.06 °C/summer). The part of the linear trend not explained by the analogues results from the global warming. The global warming gauged here by the global annual 2 m temperature from the NCEP-NCAR reanalysis represents 27 % (resp. 31 %) of the NCEP-NCAR based 1993–2012 (resp. 1983–2012) JJA T700 linear increase. A similar ratio is also found in the ECMWF reanalysis though this time series is not homogeneous over the whole period (see Supplement). By adding the global annual 2 m temperature anomalies (in respect to 1961–1990) to the analogues based T700 time series, we explain 97 ± 4 % (resp. 98 ± 5 %) of the NCEP-NCAR based T700 warming. Without applying a 10-yr running mean to the time series, the reconstructions explain 91 % (resp. 97 %) of the NCEP-NCAR based T700 warming over 1993–2012 (resp. 1983–2012).

By adding the "anthropogenic" signal to the analogues-based signal induced by changes in the general circulation, we are able to reconstruct most of the current JJA T700 variability over Greenland. However, since the state of the atmosphere is unique every day, using analogues from the past for explaining the current climate has limitations and cannot reproduce all the behaviours of the recent exceptional summers.

6 Circulation changes and global warming

The use of reanalyses instead of direct observations for detecting changes in surface melt over Greenland may be regarded as perhaps somewhat questionable (Screen and Simmonds, 2011). However, in agreement with Graversen et al. (2008) and Hanna et al. (2012), our results suggest an important role of the general circulation in the recent GrIS record surface melt, independently of global warming and Arctic amplification (Serreze et al., 2009). Nevertheless, these

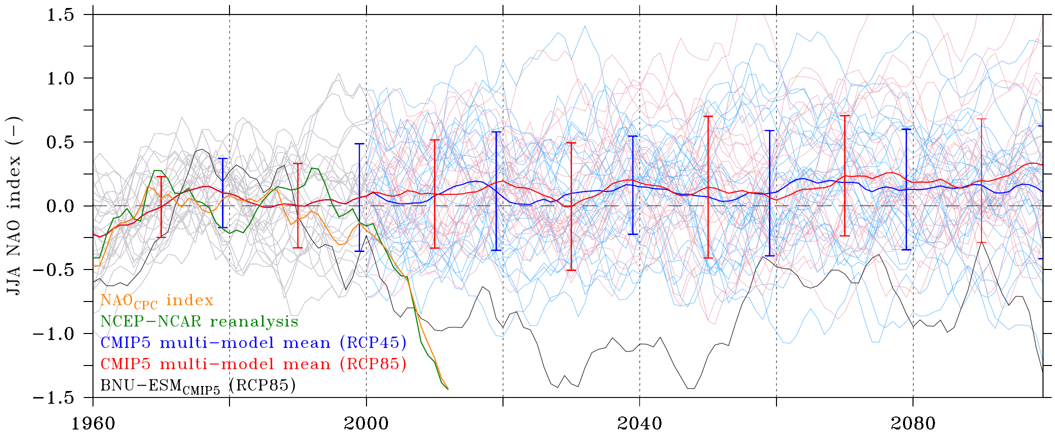

Fig. 4. Time series (10-yr running mean) of the JJA NAO index over 1960–2100. For the NCEP-NCAR reanalysis (in green) and the General Circulation Models (GCMs) from the CMIP5 database, the JJA NAO index is estimated as the standardized (over 1961–1990) difference of the JJA mean sea-level pressure between the Azores (27° W, 39° N) and Southwest Iceland (22° W, 64° N). For the CMIP5 GCMs, the historical scenario (in grey) is used for recent (1960–2005) climate conditions and future projections over 2006–2100 use RCP 4.5 (in blue) and RCP 8.5 (in red) scenarios (Moss et al., 2010). The CMIP5 multi-model mean (composed of 28 GCMs) as well as the standard deviation of the ensemble mean are also plotted in dark blue and red, respectively. The NAO time series simulated by the Chinese model BNU-ESM (using RCP8.5) is plotted in black. Finally, the JJA NAO index from CPC is plotted in orange for comparison.

recent changes in the circulation regimes could be an indirect consequence of climate change.

Indeed, Overland and Wang (2010) and Jaiser et al. (2012) showed that the recently observed sea ice retreat attributed in part to global warming (Serreze et al., 2007) influences the NAO modes in winter. In addition, observational evidence for 2007–2012 suggests there may be a link between Arctic sea-ice loss and enhanced high pressure over Greenland (Overland et al., 2012). Nevertheless, Fig. 4 seems to suggest that global warming projected by general circulation models (GCMs) from the CMIP5 (Coupled Model Intercomparison Project Phase 5) database does not greatly impact the, NAO and general circulation in summer over Greenland as shown by Belleflamme et al. (2012). While we observe a sharp decrease of the NAO index over the last 10 yr, only one GCM (plotted in black in Fig. 4) projects such negative NAO values in future and the CMIP5 ensemble mean (composed of 28 GCMs listed in Supplement) rather projects a small NAO increase for both mid-range (RCP 4.5) and high-range (RCP 8.5) scenarios through this century (see Fig. 4). It has to be noted that most of CMIP5 GCMs are able to simulate the 1961–1990 variability of the JJA NAO index, including extreme negative values as currently observed (see the Supplement). However, these models fail to simulate the current succession of summers with negative JJA NAO index values. Therefore, how the future circulation regimes will be modified by ongoing climate change remains unclear and so this whole area needs much further research. In addition, the recent changes towards a more negative summer NAO are quite short-term in the climate context and could still yet be attributed to the “natural” variability. This could explain why the GCMs do not project significant changes in NAO.

7 Conclusions

With the help of a CTC, we have shown that anticyclonic conditions (at the surface and in altitude) gauged by negative NAO indexes are twice as frequent in the last summers over Greenland compared with the last 50 yr. These anticyclones favour warmer conditions over Greenland and in particular along its western coast and the neighbouring CAA, where they induce a northward flux. Over Svalbard, the Greenland centred anticyclones tend to induce a southward flux instead. This explains why no melt increase has recently been observed over this region. By using a flow analogues method, we have estimated that these changes in the general circulation account for 69 ± 5 % (65 ± 5 %) of the 1993–2012 (resp. 1983–2012) summer warming simulated by the NCEP-NCAR reanalysis at 700 hPa over Greenland. The CMIP5 GCMs seem to suggest that these atmospheric circulation anomalies result from natural variability and not from global warming.

The next step will be to study in more depth the impact of a warmer climate on the general circulation as well as to evaluate the role played by the general circulation in the current warming observed at the whole-Arctic scale (Graversen et al., 2008; Serreze et al., 2009).

Supplementary material related to this article is available online at: http://www.the-cryosphere.net/7/241/2013/tc-7-241-2013-supplement.pdf.

Acknowledgements. Xavier Fettweis is a postdoctoral researcher of the Belgian National Fund for Scientific Research and this work was partly funded by the ANR CEPS "Green Greenland" project. We thank the European Centre for Medium-Range Weather Forecasts (ECMWF) for the ERA-40/ERA-INTERIM reanalysis (http://www.ecmwf.int), the NOAA/OAR/ESRL PSD (Boulder, Colorado, US) for the NCEP/NCAR Reanalysis (http://www.esrl.noaa.gov/psd/), the NOAA Climate Prediction Center for its NAO index (http://www.cpc.ncep.noaa.gov/) and the Climate Research Unit (CRU) for its NAO index (http://www.cru.uea.ac.uk/). For their roles in producing, coordinating, and making available the CMIP5 model output (http://cmip-pcmdi.llnl.gov/cmip5/), we acknowledge the climate modelling groups (listed in Supplement), the World Climate Research Programme's (WCRP) Working Group on Coupled Modelling (WGCM), and the Global Organization for Earth System Science Portals (GO-ESSP). Finally, we thank Jan Lenaerts and Nicole-Jeanne Schlegel for their very useful and constructive reviews which greatly improved our paper.

Edited by: E. Larour

References

Bamber, J. L., Krabill, W., Raper, V., Dowdeswell, J. A., and Oerlemans, J.: Elevation changes measured on Svalbard glaciers and ice caps from airborne laser data, Ann. Glaciol., 42, 202–208, 2005.

Belleflamme, A., Fettweis, X., Lang, C., and Erpicum, M.: Current and future atmospheric circulation at 500 hPa over Greenland simulated by the CMIP3 and CMIP5 global models, Clim. Dynam., doi:10.1007/s00382-012-1538-2, 2012.

Box, J. E., Fettweis, X., Stroeve, J. C., Tedesco, M., Hall, D. K., and Steffen, K.: Greenland ice sheet albedo feedback: thermodynamics and atmospheric drivers, The Cryosphere, 6, 821–839, doi:10.5194/tc-6-821-2012, 2012.

Chylek, P., Box, J., and Lesins, G.: Global warming and the Greenland ice sheet, Clim. Change, 63, 201–221, doi:10.1023/B:CLIM.0000018509.74228.03, 2004.

Comiso, C., Parkinson, C. L., Gerttsen, R., and Stock, L.: Accelerated decline in the Arctic sea ice cover, Geophys. Res. Lett., 35, 01703, doi:10.1029/2007GL031972, 2008.

Dee, D. P., Uppala, S. M., Simmons, A. J., Berrisford, P., Poli, P., Kobayashi, S., Andrae, U., Balmaseda, M. A., Balsamo, G., Bauer, P., Bechtold, P., Beljaars, A. C. M., van de Berg, L., Bidlot, J., Bormann, N., Delsol, C., Dragani, R., Fuentes, M., Geer, A. J., Haimberger, L., Healy, S. B., Hersbach, H., Hòlm, E. V., Isaksen, L., Kållberg, P.; Köhler, M., Matricardi, M., McNally, A. P., Monge-Sanz, B. M., Morcrette, J.-J., Park, B.-K., Peubey, C., de Rosnay, P., Tavolato, C., Thépaut, J.-N., and Vitart, F.: The ERA-Interim reanalysis: configuration and performance of the data assimilation system, Quart. J. R. Meteorol. Soc., 137, 553–597, 2011.

Fettweis, X.: Reconstruction of the 1979–2006 Greenland ice sheet surface mass balance using the regional climate model MAR, The Cryosphere, 1, 21–40, doi:10.5194/tc-1-21-2007, 2007.

Fettweis, X., Gallée, H., Lefebre, L. and van Ypersele, J.-P.: The 1988–2003 Greenland ice sheet melt extent by passive microwave satellite data and a regional climate model, Clim. Dynam., 27, 531–541, doi:10.1007/s00382-006-0150-8, 2006.

Fettweis, X., Mabille, G., Erpicum, M., Nicolay, S., and van den Broeke, M.: The 1958–2009 Greenland ice sheet surface melt and the mid-tropospheric atmospheric circulation, Clim. Dynam., 36, 139–159, doi:10.1007/s00382-010-0772-8, 2011a.

Fettweis, X., Tedesco, M., van den Broeke, M., and Ettema, J.: Melting trends over the Greenland ice sheet (1958–2009) from spaceborne microwave data and regional climate models, The Cryosphere, 5, 359–375, doi:10.5194/tc-5-359-2011, 2011b.

Fettweis, X., Franco, B., Tedesco, M., van Angelen, J. H., Lenaerts, J. T. M., van den Broeke, M. R., and Gallé, H.: Estimating Greenland ice sheet surface mass balance contribution to future sea level rise using the regional atmospheric climate model MAR, The Cryosphere Discuss., 6, 3101–3147, doi:10.5194/tcd-6-3101-2012, 2012.

Fisher, D., Zheng, J., Burgess, D., Zdanowicz, C., Kinnard, C., Sharp, M., and Bourgeois, J.: Recent melt rates of Canadian arctic ice caps are the highest in four millennia, Global Planet. Change, 84–85, 3–7, doi:10.1016/j.gloplacha.2011.06.005, 2012.

Gardner, A. S., Moholdt, G., Wouters, B., Wolken, G. J., Burgess, D. O., Sharp, M. J., Cogley, J. G., Braun, C., and Labine, C.: Sharply increased mass loss from glaciers and ice caps in the Canadian Arctic Archipelago, Nature, 473, 357–360, doi:10.1038/nature10089, 2011.

Graversen, R. G., Mauritsen, T., Tjernstrom, M., Kallen, E., and Svensson, G.: Vertical structure of recent Arctic warming, Nature, 451, 7174, 53–56, doi:10.1038/nature06502, 2008.

Hanna, E., Huybrechts, P., Steffen, K., Cappelen, J., Huff, R., Shuman, C., Irvine-Fynn, T., Wise, S., and Griffiths, M.: Increased runoff from melt from the Greenland ice sheet: a response to global warming, J. Climate, 21, 331–341, 2008.

Hanna, E., Jones, J. M., Cappelen, J., Mernild, S. H., Wood, L., Steffen, K., and Huybrechts, P.: The influence of North Atlantic atmospheric and oceanic forcing effects on 1900–2010 Greenland summer climate and ice melt/runoff, Int. J. Climatol., doi:10.1002/joc.3475, 2012a.

Hanna, E., Mernild, S. H., Cappelen, J., and Steffen, K.: Recent warming in Greenland in a long-term instrumental (1881–2012) climatic context: I. Evaluation of surface air temperature records, Environ. Res. Lett., 7, 045404, doi:10.1088/1748-9326/7/4/045404, 2012b.

Jaiser, R., Dethloff, K., Handorf, D., Rinke, A., and Cohen, J.: Impact of sea ice cover changes on the Northern Hemisphere atmospheric winter circulation, Tellus, 64, 11595, doi:10.3402/tellusa.v64i0.11595, 2012.

Kalnay, E., Kanamitsu, M., Kistler, R., Collins, W., Deaven, D., Gandin, L., Iredell, M., Saha, S., White, G., Woollen, J., Zhu, Y., Leetmaa, A., Reynolds, B., Chelliah, M., Ebisuzaki, W., Higgins, W., Janowiak, J., Mo, K., Ropelewski, C., Wang, J., Jenne, R., and Joseph, D.: The NCEP/NCAR 40 year reanalysis project, B. Am. Meteorol. Soc., 77, 437–471, 1996.

Kvamsto, N. G., Steinskog, D. J., Stephenson, D. B., and Tjostheim, D. B.: Estimation of trends in extreme melt-season duration at Svalbard, Int. J. Climatol., 32, 2227–2239, doi:10.1002/joc.3395, 2012.

Lund, I. A.: Map-pattern typeification by statistical methods. J. Appl Meterol., 2, 56–65, 1963.

Moholdt, G., Nuth, C., Hagen, J. O., and Köhler, J.: Recent elevation changes of Svalbard glaciers derived from ICESat laser altimetry, Remote Sens. Environ., 114, 2756–2767, doi:10.1016/j.rse.2010.06.008, 2010.

Moss, R. H., Edmonds, J. A., Hibbard, K., Manning, M., Rose, S. K., van Vuuren, D. P., Carter, T. R., Emori, S., Kainuma, M., Kram, T., Meehl, G., Mitchell, J., Nakicenovic, N., Riahi, K., Smith, S., Stouffer, R. J., Thomson, A., Weyant, J., and Wilbanks, T.: The next generation of scenarios for climate change research and assessment, Nature, 463, 747–756, 2010.

Mote, T. L.: Mid-tropospheric Circulation and surface melt on the Greenland ice sheet, Part 1, Int. J. Climatol., 18, 111–130, 1998.

Mote, T. L.: Greenland surface melt trends 1973–2007: evidence of a large increase in 2007, Geophys. Res. Lett., 34, L22507, doi:10.1029/2007GL031976, 2007.

Overland, J. E. and Wang, M.: Large-scale atmospheric circulation changes are associated with the recent loss of Arctic sea ice, Tellus A, 62, 1–9, doi:10.1111/j.1600-0870.2009.00421.x, 2010.

Overland, J. E., Francis, J., Hanna, E., and Wang, M.: The recent shift in early summer arctic atmospheric circulation, Geophys. Res. Lett., 39, L19804, doi:10.1029/2012GL053268, 2012.

Philipp, A., Bartholy, J., Beck, C., Erpicum, M., Esteban, P., Fettweis, X., Huth, R., James, P., Jourdain, S., Kreienkamp, F., Krennert, T., Lykoudis, S., Michalides, S., Pianko, K., Post, P., Rassilla Álvarez, D., Schiemann, R., Spekat, A., and Tymvios, F. S.: COST733CAT – a database of weather and circulation type classifications, Phys. Chem. Earth, 35, 360–373, 2010.

Rignot, E. I., Velicogna, van den Broeke, M. R., Monaghan, A., and Lenaerts, J.: Acceleration of the contribution of the Greenland and Antarctic ice sheets to sea level rise, Geophys. Res. Lett., 38, 05503, doi:10.1029/2011GL046583, 2011.

Screen, J. and Simmonds, I.: Erroneous Arctic temperature trends in the ERA-40 reanalysis: a closer look, J. Climate, 24, 2620–2627, doi:10.1175/2010JCLI4054.1, 2011.

Serreze, M., Holland, M., and Stroeve, J.: Perspectives on the Arctic's shrinking sea-ice cover, Science, 315, 1533–1536, doi:10.1126/science.1139426, 2007.

Serreze, M. C., Barrett, A. P., Stroeve, J. C., Kindig, D. N., and Holland, M. M.: The emergence of surface-based Arctic amplification, The Cryosphere, 3, 11–19, doi:10.5194/tc-3-11-2009, 2009.

Sharp, M., Burgess, D. O., Cogley, J. G., Ecclestone, M., Labine, C., and Wolken, G. J: Extreme melt on Canada's Arctic ice caps in the 21th century, Geophys. Res. Lett., 38, 11501, doi:10.1029/2011GL047381, 2011.

Tedesco, M., Serreze, M., and Fettweis, X.: Diagnosing the extreme surface melt event over southwestern Greenland in 2007, The Cryosphere, 2, 159–166, doi:10.5194/tc-2-159-2008, 2008a.

Tedesco, M., Fettweis, X., van den Broeke, M. R., van de Wal, R. S. W., and Smeets, C. J. P. P.: Extreme snowmelt in Northern Greenland during summer 2008, Eos Trans. AGU, 89, 391–391, doi:10.1029/2008EO410004, 2008b.

Tedesco, M., Fettweis, X., van den Broeke, M., van de Wal, R., Smeets, P., van de Berg, W. J., Serreze, M., and Box, J.: The role of albedo and accumulation in the 2010 melting record in Greenland, Environ. Res. Lett., 6, 014005, 1–6, doi:10.1088/1748-9326/6/1/014005, 2011.

Tedesco, M., Fettweis, X., Mote, T., Wahr, J., Alexander, P., Box, J., and Wouters, B.: Evidence and analysis of 2012 Greenland records from spaceborne observations, a regional climate model and reanalysis data, The Cryosphere Discuss., 6, 4939–4976, doi:10.5194/tcd-6-4939-2012, 2012.

Uppala, S. M., Kållberg, P. W., Simmons, A. J., Andrae, U., da Costa Bechtold, V., Fiorino, M., Gibson, J. K., Haseler, J., Hernandez, A., Kelly, G. A., Li, X., Onogi, K., Saarinen, S., Sokka, N., Allan, R. P., Andersson, E., Arpe, K., Balmaseda, M. A., Beljaars, A. C. M., van de Berg, L., Bidlot, J., Bormann, N., Caires, S., Chevallier, F., Dethof, A., Dragosavac, M., Fisher, M., Fuentes, M., Hagemann, S., Hòlm, E., Hoskins, B. J., Isaksen, L., Janssen, P. A. E. M., Jenne, R., McNally, A.P., Mahfouf, J.-F., Morcrette, J.-J., Rayner, N. A., Saunders, R. W., Simon, P., Sterl, A., Trenberth, K. E., Untch, A., Vasiljevic, D., Viterbo, P., and Woollen, J.: The ECMWF re-analysis, Q. J. Roy. Meteor. Soc., 131, 2961–3012, doi:10.1256/qj.04.176, 2005.

Van den Broeke, M. R., Bamber, J., Ettema, J., Rignot, E., Schrama, E., van de Berg, W. J., van Meijgaard, E., Velicogna, I., and Wouters, B.: Partitioning recent Greenland mass loss, Science, 326, 984–986, 2009.

Vautard, R. and P. Yiou: Control of recent European surface climate change by atmospheric flow, Geophys. Res. Lett., 36, 22702, doi:10.1029/2009GL040480, 2009.